Available online at www.sciencedirect.com
ScienceDirect
Journal of Non-Crystalline Solids 352 (2006) 3244–3248
JOURNAL OF NON-CRYSTALLINE SOLIDS
www.elsevier.com/locate/jnoncrysol

Phase formation and physical properties of mechanically alloyed amorphous 55Mg35Ni10Si

Dengke Yang [a], Cui'e Wen [b], Fusheng Han [a,*], Yujie Yang [a]

[a] Key Laboratory of Materials Physics, Institute of Solid State Physics, Chinese Academy of Sciences, Hefei, Anhui 230031, China
[b] School of Engineering and Technology, Deakin University, Geelong, Vic. 3217, Australia

Received 19 October 2005; received in revised form 27 April 2006

Abstract

Amorphous 55Mg35Ni10Si alloy powder has been synthesized by mechanical alloying technique using pure Mg, Ni and Si elemental powders. The transformation of the crystalline powders into an amorphous one has been investigated by X-ray diffraction, scanning electron microscopy, transmission electron microscopy and differential scanning calorimetry. The new material produced has a higher thermal stability than reported results, which is beneficial to the fabrication of Mg–Ni–Si bulk amorphous components through powder metallurgy.

PACS: 61.43.Dq; 81.05.Zx; 81.20.Ev

Keywords: Amorphous metals; Metallic glasses; Alloys; Mechanical alloying; Crystallization; Glass formation; Microstructure

1. Introduction

Mg alloys are well known light-weight alloy systems with outstanding specific mechanical properties that will find applications in a number of engineering fields [1]. Unfortunately, the plasticity and the toughness of Mg alloys are usually unsatisfactory and therefore, implementation treatments have to be conducted to improve these properties. As is widely reported, metallic materials with nano-grains show extraordinary physical and mechanical properties and this suggests that the plasticity and the toughness of the Mg alloys can be modified if the grains are tailored into nanometer dimensions. Among others, amorphous route has been proved to be one of the most effective technologies in producing nanocrystalline structures through crystallization [2–6]. There are several ways to produce Mg based amorphous alloys including mechanical alloying (MA) [7–9]. The main Mg based amorphous ternary alloy powders prepared via MA include Mg–Y–Cu [10,11], Mg–Ni–Ge [12], Mg–Ni–Sn [13], Mg–Ni–Y [14,15], and Mg–Al–Ca [16]. The selection of ternary alloy system may be based on the fact that they have relatively strong glass formation ability in comparison of binary alloys [17]. However, although these Mg ternary systems have very strong glass forming ability, they have relatively low crystallization temperatures, which is unfavorable for production of bulk amorphous component through hot pressing or extrusion. It has been proved that Ni has a rather high amorphous forming ability and Si tends to elevate the glass transition temperature of Mg based amorphous materials, and thus elemental Mg, Ni and Si powders were selected as starting materials in the present study. The MA processing parameters and alloy compositions were investigated with the objective of fabricating a new ternary Mg based amorphous powder with a relatively high crystallization temperature. It is expected that the new ternary Mg–Ni–Si amorphous alloy powder will be suitable for developing bulk amorphous components that will be useful in automobile parts, portable electric appliances,

* Corresponding author. Tel.: +86 551 5591435; fax: +86 551 5591434.
E-mail address: fshan@issp.ac.cn (F. Han).

0022-3093/$ - see front matter © 2006 Elsevier B.V. All rights reserved.
doi:10.1016/j.jnoncrysol.2006.05.027

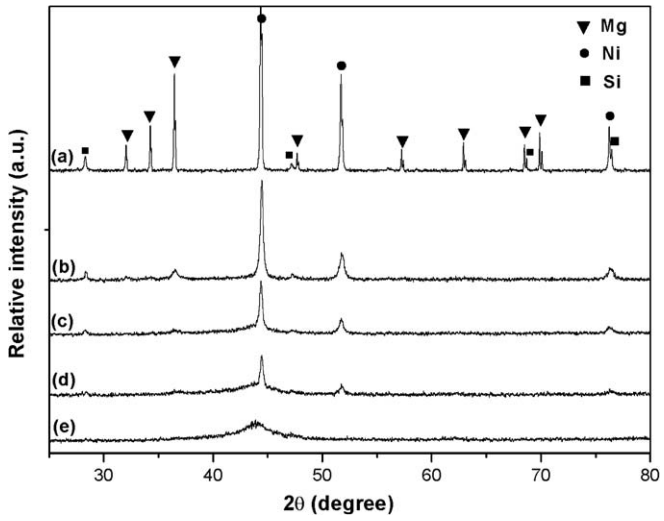

Fig. 1. XRD patterns of 55Mg35Ni10Si powder after milling for (a) 0 h; (b) 20 h; (c) 30 h; (d) 44 h and (e) 68 h.

aerospace components, sports equipment and hydrogen storage applications and so on.

2. Experimental procedure

The starting materials are elemental Mg, Ni and Si powders with the purity of 99.9% and the nominal mean diameters of the powders are 180 μm, 35 μm and 44 μm, respectively. The powders were weighed using an electrical balance with an accuracy of 0.01 g in terms of the targeted composition of 55Mg35Ni10Si in atom percent. The mixtures of 20 g starting powders and 400 g stainless steel balls with a diameter of 10 mm were used in each milling test. It has been known that the powder particulates tend to bind together after milling for a certain time, giving rise to so called cold-welding effect due to heavy plastic deformation of the metallic particulates, such as Mg and Ni particulates in the present study. To weaken the cold-welding effect, 2 wt% stearic acid was added into the powder mixtures before the milling [7]. The MA was conducted in a Retsch mill (PM400), where the pot rotates against the revolution and cold air is blown over the pot to keep the pot from heating up. The rotation speed was 200 rpm and the milling time ranged from 20 to 68 h. During the milling, the powders are liable to adhere to the wall of the pot due to the so called cold welding effect, causing the milling efficiency decreased or even uncompleted milling. The pot was therefore taken into a glove box every 5 h to remove the adherent powders from the pot wall and to break the agglomerated powders. Meanwhile, a small amount of powders were taken out from the pot to examine the evolution of the microstructures of the milled powders. The phase composition of the milled powders was characterized by X-ray diffraction (XRD) using Cu Kα radiation (X′ Pert Pro MPD) and the thermal stability was evaluated by differential scanning calorimetry (DSC, Pyris Diamond) at a heating rate of 20 K/min under argon atmosphere. The microstructures were examined by high resolution transmission electron microscopy (HRTEM, Philips JEM2010) and scanning electron microscopy (SEM, Leica S440).

3. Results

Fig. 1 shows the typical XRD spectra of the 55Mg35Ni10Si alloy powders milled for different times from 20 to 68 h. For the initial mixture of the powders, sharp diffraction peaks related to hcp-Mg, fcc-Ni and fcc-Si appeared in the spectrum. These peaks gradually became lower and broader and some peaks even disappeared with increasing milling time, as shown in Fig. 1(b) and (c), due to the refinement of the crystalline grains and increase of lattice strain. With further increasing milling time such as milling for 44 h, however, only small Ni peaks can be seen while the Mg and Si related peaks are almost invisible. This phenomenon should not be attributed to the dissolution of Mg and Si in Ni because the Ni diffraction peaks did not shift [18]. In order to understand the state of Mg and Si at this stage, the powders milled for 44 h were analyzed by HRTEM, as shown by the bright field image and the diffraction pattern in the selected area in Fig. 2(a) and

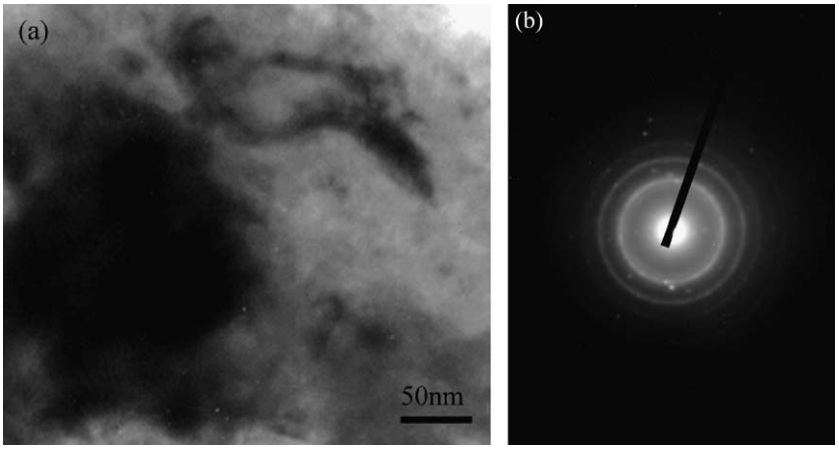

Fig. 2. (a) Bright field image and (b) diffraction pattern of the selected area for the 55Mg35Ni10Si powder after milling for 44 h.

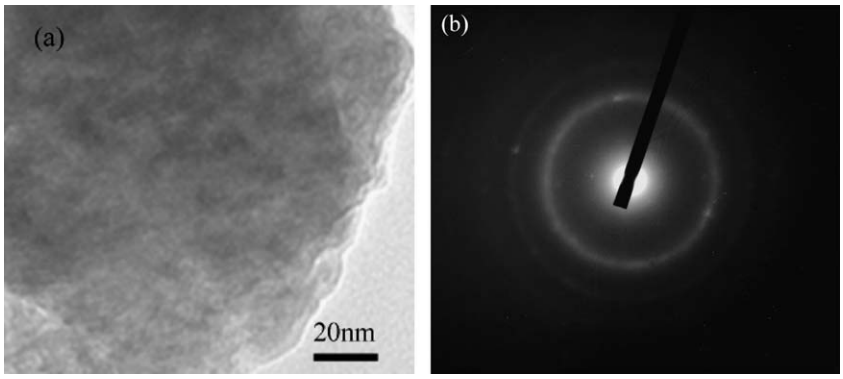

Fig. 3. (a) Bright field image and (b) diffraction pattern of the selected area for the 55Mg35Ni10Si powder after milling for 68 h.

(b). It is seen that, in addition to the sharp diffraction rings and some bright spots, a diffusive diffraction ring presented near the center, showing the existence of an amorphous phase. Therefore, the most of Mg, Si and some Ni have transformed into the amorphous phase in this stage. As the milling proceeded, the amount of the amorphous phase increased until a single amorphous phase was achieved, as shown by the broad peak shown in Fig. 1(e). The corresponding bright field image and the selected area diffraction pattern shown in Fig. 3(a) and (b) further evidence the formation of the single amorphous phase. The particulates show a very fine and homogeneous microstructure without any facet structure, and the diffusive halo with limited diffraction spots shows a typical amorphous feature, being in good agreement with the XRD results presented in Fig. 1(e).

4. Discussion

It is useful to compare the above MA results with those of conventional solid state reactions induced by thermal annealing of the same premilled powders. Fig. 4 shows DSC curves of the 55Mg35Ni10Si powders milled for 20, 44 and 68 h, illustrating the differences among the three powders. The powder milled for 20 h exhibited a broad endothermic peak at about 260 °C, while the powder milled for 44 h not only showed a smaller endothermic peak at an elevated temperature, but also exhibited a sharp exothermic peak at around 410 °C. For the powder milled for 68 h, however, only a sharp exothermic peak appeared at 420 °C and no endothermic peak can be seen. In order to understand the origin of these peaks, XRD measurements were performed with the powders milled for 20 h and 68 h, as shown in Figs. 5 and 6. For the powder milled for 20 h, there only existed the peaks of Ni, Si and Mg_2Si in the original powder, while there existed enhanced Si and Ni peaks and other peaks related to compounds such as Mg_2Si, Mg_5Si_6, $MgNi_2$, and Mg_2Ni_3Si in the heat treated powder. The enhanced Si and Ni peaks can be attributed to the growth of crystal grains during the heat treatment, and the formation of new phases is most likely due to the inhomogeneous mixing of the milled powders. From the above XRD results, the endothermic peak at 260 °C should be related to layer bonding by atomic diffu-

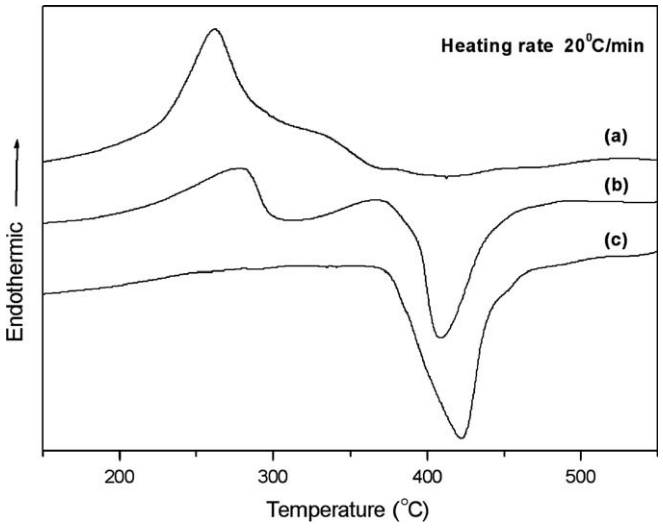

Fig. 4. DSC curves of the 55Mg35Ni10Si powder after milling for (a) 20 h; (b) 44 h and (c) 68 h.

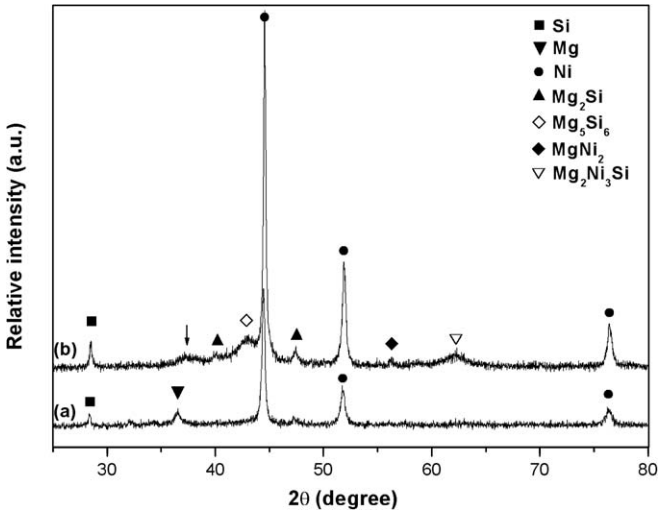

Fig. 5. XRD patterns of (a) without heat treatment and (b) heat treated to 300 °C at a heating rate of 20 K/min for the 55Mg35Ni10Si powder after milling for 20 h.

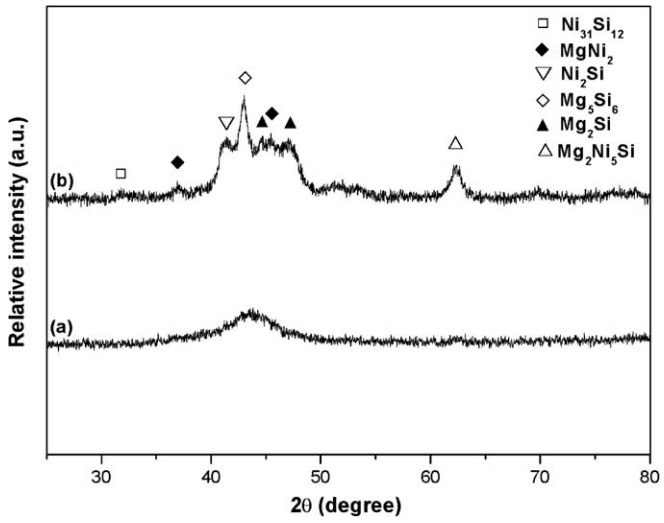

Fig. 6. XRD patterns of (a) without heat treatment and (b) heat treated to 500 °C at a heating rate of 20 K/min for the 55Mg35Ni10Si powder after milling for 68 h.

sion in the solid state that resulted in the formation of these compounds and the growth of Si and Ni crystal grains. In addition, it is seen from the XRD pattern in Fig. 5 that all diffraction peaks of the resultant phases are broader and lower than those of the corresponding peaks of the powders without MA and heat treatment, suggesting that the 20 h milling had lead to the formation of nanocrystalline and amorphous grains, as indicated by the arrow in Fig. 5(b). It is noted that some powders have agglomerated to form as large as 15–20 μm particulates due to the cold welding effect during the MA, as shown in Fig. 7. After 68 h milling, large differences in the XRD patterns were noted between the heat treated and original powders. The XRD pattern of the powder after heat treatment reveals the appearance of some new phases, which are nanocrystalline $Mg_{31}Si_{12}$, Mg_2Si, Mg_5Si_6, $MgNi_2$, Mg_2Ni_5Si and Ni_2Si.

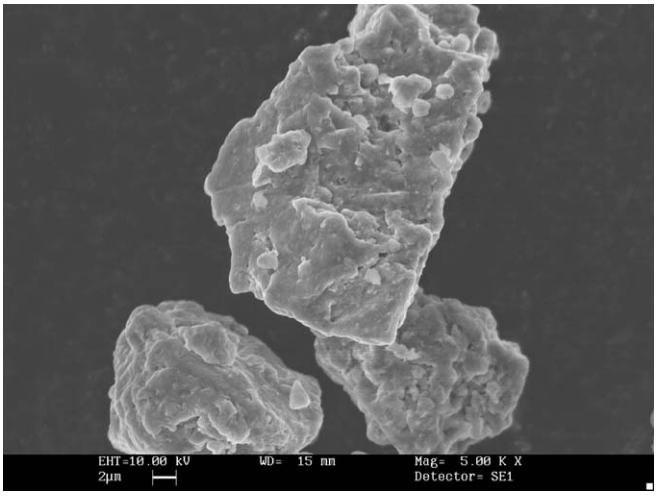

Fig. 7. SEM micrograph of typical 55Mg35Ni10Si agglomerates after milling for 20 h.

Accordingly, the exothermic peak at 420 °C should be attributed to the crystallization of the amorphous phase. It should be pointed out that this temperature is much higher than reported values, for example, 300 °C for 75Mg15Ni10Si powder, which is due to the relatively high Si/Mg ratio in the present powders [19]. As mentioned above, relatively high crystallization temperature is extremely important for manufacturing bulk amorphous components because the consolidation of the amorphous powders is usually conducted at relatively high temperatures during extrusion. The elevated crystallization temperature of the amorphous powders is necessary to guarantee the amorphous microstructures after consolidation [20].

As displayed in Fig. 2(a), heavy and heterogeneous plastic deformation arisen in the powders and in the diffraction pattern at the selected zone shown in Fig. 2(b), the bright Laue spots suggest that the oriented particles have very fine crystalline grains in the unprocessed Ni. In addition, the diffusive diffraction rings demonstrate the occurrence of the amorphous phase. It is in good agreement with the DSC results shown in Fig. 4(b), where the first endothermic peak is caused by the reaction of the unprocessed Mg, Ni and Si powders to form the new phases. The physical significance of the observed exothermic peak lies in that it actually represents the crystallization temperature of the amorphous powder. Increasing the milling time leads to decreased amount of the unprocessed Mg, Ni and Si and thus gives rise to increased amount of the amorphous phase. Moreover, the enthalpy ΔH of the endothermic peak for the powder milled for 44 h is smaller than that milled for 20 h, while the enthalpy ΔH of the exothermic peak for the powder milled for 44 h is smaller than that milled for 68 h. These differences are consistent with the crystallization temperatures of the powders having varied milling times and also disclose the evolution of the microstructures in the amorphous phases.

The experimental results reveal the influence of milling time on both the evolution of the phases and the final product of 55Mg35Ni10Si powders. After a relatively short milling, for example 20 h, the powders were transformed into layered structures and refined crystalline grains, as demonstrated by the broadened diffraction peaks in the XRD spectra. With increasing milling time, a solid state reaction must have taken place that caused some powders to transform into amorphous phase in addition to nanocrystalline phases. Finally, when the milling time reached 68 h, the solid state reaction was complete and most of the powders were transformed into the 55Mg35Ni10Si amorphous phase. It is therefore concluded that the microstructures of the powders developed during the MA should be in the order of the grain refinement, the formation of the amorphous Mg and Si and the formation of the amorphous 55Mg35Ni10Si alloy, as shown by the following reactions:

$$\mathrm{Mg}+\mathrm{Ni}+\mathrm{Si}\rightarrow \mathrm{Mg}_{\mathrm{nanocrystalline}}+\mathrm{Ni}_{\mathrm{nanocrystalline}}+\mathrm{Si}_{\mathrm{nanocrystalline}} \rightarrow (\mathrm{Mg–Ni–Si})_{\mathrm{amorphous}}+\mathrm{Ni}_{\mathrm{nanocrystalline}}\rightarrow (55\mathrm{Mg35Ni10Si})_{\mathrm{amorphous}}$$

5. Conclusions

Amorphous 55Mg35Ni10Si powders were produced by mechanical alloying technique. The sequence of phase transformations during the milling can be described as follows:

$$\begin{aligned}\mathrm{Mg}+\mathrm{Ni}+\mathrm{Si} &\rightarrow \mathrm{Mg}_{\mathrm{nanocrystalline}}+\mathrm{Ni}_{\mathrm{nanocrystalline}}+\mathrm{Si}_{\mathrm{nanocrystalline}}\\ &\rightarrow (\mathrm{Mg–Ni–Si})_{\mathrm{amorphous}}+\mathrm{Ni}_{\mathrm{nanocrystalline}}\\ &\rightarrow (\mathrm{55Mg35Ni10Si})_{\mathrm{amorphous}}\end{aligned}$$

The amorphous powder has a relatively high thermal stability. The crystallization temperature of the powder is as high as 380 °C, which is beneficial to the consolidation of bulk amorphous materials. These results show promise towards the development of Mg–Ni–Si amorphous alloys through powder metallurgy.

Acknowledgement

This work is financially supported by The Natural Science Foundation of Anhui, China under the Contract of 050440601.

References

[1] B.L. Mordike, U. Kainer, Proceedings of the Conference on Magnesium Alloys and Their Applications, Wolfsburg, Germany, 1998.
[2] G.L. Song, A. Atrens, Adv. Eng. Mater. 5 (2003) 837.
[3] B.L. Mordike, J. Mater. Proc. Technol. 117 (2001) 391.
[4] H. Watanabe, T. Mukai, M. Mabuchi, K. Higashi, Acta Mater. 49 (2001) 2027.
[5] A. Inoue, H. Kimura (Eds.), Proceedings of the 22nd Risø International Symposium on Materials Science: Science of Metastable and Nanocrystalline Alloys Structure, Properties and Modelling, Risø National Laboratory, Roskilde, Denmark, 2001.
[6] M. Sherif El-Eskandarany, Mechanical Alloying for Fabrication of Advanced Engineering Materials, Noyes Publications/William Andrew Publishing, Norwich, NY, USA, 2001, p. 1.
[7] C. Suryanarayana, Prog. Mater. Sci. 41 (2001) 1.
[8] G.M. Dougherty, G.J. Shiflet, S.J. Poon, Acta Mater. 42 (1994) 2275.
[9] J. Eckert, Mater. Sci. Eng. A 364 (1997) 226.
[10] M. Seidel, J. Echkert, E. Zueco-Rodrigo, L. Schultz, J. Non-Cryst. Solids 205–207 (1996) 514.
[11] N. Schlorke, B. Weiss, J. Echert, L. Schultz, Nano Struct. Mater. 12 (1999) 127.
[12] F.C. Gennari, G. Urretavizcaya, J.J. Andrade Gamboa, G. Meyer, J. Alloy. Compd. 354 (2003) 187.
[13] S.Y. Su, Y. He, G.J. Shiflet, S.J. Poon, Mater. Sci. Eng. A 185 (1994) 115.
[14] Y.M. Soifer, N.P. Kobelev, I.G. Brodova, A.N. Manukhin, E. Korin, L. Soifer, Nano Struct. Mater. 12 (1999) 875.
[15] K. Ozaki, K. Kobayashi, A. Sugiyama, T. Nishio, A. Matsumoto, J. Powder Metall. 47 (2000) 423.
[16] L.E. Hazelton, C.A. Nielsen, U.V. Deshmukh, P.E. Pierini, in: F.H. Froes, J.J. deBarbadillo (Eds.), Structural Applications of Mechanical Alloying., ASM International, OH, Materials Park, 1990.
[17] W.H. Wang, C. Dong, C.H. Shek, Mater. Sci. Eng. R 44 (2004) 45.
[18] J.Y. Huang, L.L. Ye, Y.K. Wu, H.Q. Ye, Acta Mater. 44 (1996) 1781.
[19] K. Ozaki, T. Nishio, A. Matsumoto, K. Kobayashi, Mater. Sci. Eng. A 375–377 (2004) 857.
[20] O.N. Senkov, S.V. Senkova, J.M. Scott, D.B. Miracle, Mater. Sci. Eng. A 393 (2005) 12.